

37 atmospheric water vapor, its large dynamic range (typically 3 – 40 000 ppmv¹), and its broad spectroscopic
38 fingerprint typically require complex multi-dimensional calibrations, in particular for spectroscopic sensors.
39 These calibrations often embrace the water vapor content of the gas flow to be analyzed as one of the key
40 calibration parameters even if the instrument (e.g. for CO₂), is not intended to measure water vapor at all.

41

42 In particular for field weather stations, water vapor analyzers often are seen as part of the standard
43 instrumentation in atmospheric research. This seems reasonable due to several reasons: slow H₂O mole
44 fraction change over hours, the typical mid-range humidity levels (approx. above 5000 ppmv), no
45 significant gas pressure or temperature change, target accuracy often only in the on the order of 5-15%
46 relative deviation, and the absence of “non-typical atmospheric components” such as soot or hydrophobic
47 substances. Water vapor measurements under these conditions can be performed by a variety of different
48 devices (Wiederhold, 1997): Capacitive polymer sensors e.g. (Salasmaa and Kostamo, 1986) are frequently
49 deployed in low cost (field) applications. Small-scale produced, commercially available spectral absorption
50 devices e.g. (Petersen et al., 2010) are often used in research campaigns. Dew-point mirror hygrometers
51 (DPM) are known for their high accuracy. However, this is only true if they are regularly calibrated at high
52 accuracy (transfer-) standards in specialized hygrometry laboratories such as in metrology institutes
53 (Heinonen et al., 2012).

54 As soon as hygrometers have to be deployed in harsh environments (e.g. on airborne platforms), this
55 situation changes entirely: The ambient gas pressure (10 – 1000 hPa) and gas temperature (-90 – 40°C)
56 ranges are large and both values change rapidly, the required H₂O measurement range is set by the ambient
57 atmosphere (typically 3 – 40000 ppmv), mechanical stress and vibrations occur, and the sampled air
58 contains additional substances from condensed water (ice, droplets), particles, or even aircraft fuel vapor
59 (e.g. on ground). These and other impacts complicate reliable, accurate, long-term stable H₂O
60 measurements and briefly outline why water vapor measurements remain difficult in-situ measurements in
61 the field, even if they are nearly always needed in atmospheric science. Usually, the availability and
62 coverage of observations limit model validation studies in the first place but also the lack of sufficient
63 accuracy may have limited important scientific interpretations (Krämer et al., 2009; Peter et al., 2006; Scherer
64 et al., 2008; Sherwood et al., 2014).

65 Over the last decades, numerous hygrometers were developed and deployed on aircraft (Busen and Buck,
66 1995; Cerni, 1994; Desjardins et al., 1989; Diskin et al., 2002; Durrty et al., 2008; Ebert et al., 2000; Gurlit et al.,
67 2005; Hansford et al., 2006; Helten et al., 1998; Hunsmann et al., 2008; Karpechko et al., 2014; Kley and
68 Stone, 1978; May, 1998; Meyer et al., 2015; Ohtaki and Matsui, 1982; Roths and Busen, 1996; Salasmaa and
69 Kostamo, 1986; Schiff et al., 1994; Silver and Hovde, 1994b, 1994a; Thornberry et al., 2014; Webster et al.,
70 2004; Zöger et al., 1999a, 1999b) (non-exhaustive list). While for some atmospheric questions the quality
71 level of the data often is sufficient (e.g. typically climatologies), there are also a variety of questions,

¹ SEALDH-II native unit for H₂O concentration measurement is mole fraction. The SI conform unit would be mol/mol. We kept the ppmv (= μmol/mol) since most atmospheric communities are more used to it. For the same reason, we used the words “concentration” and “mole fraction” synonymously.

72 especially validation of atmospheric models, where the required absolute accuracy, precision, temporal
73 resolution, long-term stability, comparability, etc. needs to be higher. These problems can be grouped into
74 two major categories: accuracy linked problems and time response linked problems. The latter is
75 particularly important for investigations in heterogeneous regions in the lower troposphere as well as for
76 investigations in clouds. In these regions, even two on average agreeing instruments with different
77 response times yield local, large, relative deviations on the order of up to 30% (Smit et al., 2014). It is
78 important to keep in mind, that the total time response of a system is a superposition of the time response
79 components of the instrument itself as well as of the sampling inlet. These typically depend on numerous
80 parameters like e.g. type of inlet, inlet pipe length, pipe coating, pipe temperature, pipe heating, gas flow,
81 input air humidity level, etc..

82 In contrast to time response studies, accuracy linked problems in flight are difficult to isolate since they are
83 always covered by the spatial variability (which leads to temporal variability for moving aircraft) of
84 atmospheric H₂O distribution. Comparing hygrometer in flight, such as, for example in (Rollins et al., 2014),
85 does not facilitate a clear accuracy assessment.

86 Therefore in 2007, an international intercomparison exercise named “AquaVIT” (Fahey et al., 2014) was
87 carried out to compare airborne hygrometers under quasi-static, laboratory-like conditions for upper
88 tropospheric and lower stratospheric humidity levels. AquaVIT (Fahey et al., 2014) encompassed 22
89 instruments from 17 international research groups. The instruments were categorized in well-validated,
90 often deployed “core” instruments (APicT, FISH, FLASH, HWV, JLH, CFH) and “younger” non-core
91 instruments. AquaVIT revealed in the important 1 to 150 ppmv H₂O range, that -even under quasi-static
92 conditions- the deviation between the core instrument’s readings and their averaged group mean was on
93 the order of ± 10 %. This result fits to the typical interpretation problems of flight data where instruments
94 often deviate from each other by up to 10%, which is not covered by the respective uncertainties of the
95 individual instruments. AquaVIT was a unique first step to document and improve the accuracy of airborne
96 measurements in order to make them more comparable. However, no instrument could claim after
97 AquaVIT that its accuracy is higher than any other AquaVIT instrument, since no “gold standard” was part
98 of the campaign, i.e., a metrological transfer standard (JCGM 2008, 2008; Joint Committee for Guides in
99 Metrology (JCGM), 2009) traced back to the SI units. There is no physical argument for the average being
100 better than the measured value of a single instrument. Instead, many arguments speak for systematic
101 deviations of airborne hygrometers: Most hygrometers have to be calibrated. Even for a perfect instrument,
102 the accuracy issue is represented by the calibration source and its gas handling system, which in this case
103 leads to two major concerns: First, one has to guarantee that the calibration source is accurate and stable
104 under field conditions, i.e., when using it before or after a flight on the ground. This can be challenging
105 especially for the transportation of the source with all its sensitive electronics/mechanics and for the
106 deviating ambient operation temperature from the ambient validation temperature (hangar vs. laboratory).
107 Even more prone to deviations are calibration sources installed inside the aircraft due to changing ambient
108 conditions such as cabin temperature, cabin pressure, orientation angle of instrument (important, if liquids
109 are used for heating or cooling). Secondly, the gas stream with a highly defined amount of water vapor has

110 to be conveyed into the instrument. Especially for water vapor, which is a strongly polar molecule, this gas
111 transport can become a critical step. Changing from high to low concentrations or even just changing the
112 gas pressure or pipe temperature can lead to signal creep due to slow adsorption and desorption processes,
113 which can take long to equilibrate. In metrology, this issue is solved by a long validation/calibration time
114 (hours up to weeks, depending on the H₂O mole fraction level), a generator without any connectors/fittings
115 (everything is welded) and piping made out of electro-polished, stainless steel to ensure that the
116 equilibrium is established before the actual calibration process is started. However, this calibration
117 approach is difficult to deploy and maintain for aircraft/field operations due to the strong atmospheric
118 variations in gas pressure and H₂O mole fraction, which usually leads to a multi-dimensional calibration
119 pattern (H₂O mole fraction, gas pressure, sometimes also gas temperature) in a short amount of calibration
120 time (hours). Highly sensitive, frequently flown hygrometers like (Zöger et al., 1999b) are by their physical
121 principle, not as long-term stable as it would be necessary to take advantage of a long calibration session.
122 Besides the time issue to reach a H₂O equilibrium between source and instrument, most calibration
123 principles for water vapor are influenced by further issues. A prominent example is the saturation of air in
124 dilution/saturation based water vapor generators: gas temperature and pressure defines the saturation level
125 (described e.g. by Sonntag's Equation (Rollins et al., 2014)), however, it is well-known that e.g. 100.0%
126 saturation is not easily achievable. This might be one of the impact factors for a systematic offset during
127 calibrations in the field. The metrology community solves this for high humidity levels with large, multi-
128 step saturation chambers which decrease the temperature step-wise to force the water vapor to condense in
129 every following step. These few examples of typical field-related problems show, that there is a reasonable
130 doubt that deviations in field situations are norm-distributed. Hence, the mean during AquaVIT might be
131 biased, i.e. not the correct H₂O value.

132 The instruments by themselves might actually be more accurate than AquaVIT showed, but deficiencies of
133 the different calibration procedures (with their different calibration sources etc.) might mask this. To
134 summarize, AquaVIT documented a span of up to 20% relative deviation between the world's best airborne
135 hygrometers – but AquaVIT could not assess absolute deviations nor explain them, since a link to a
136 metrological H₂O primary standard (i.e., the definition of the international water vapor scale) was missing.
137 While AquaVIT focused primarily on the stratospheric H₂O range from 0 – 150 ppmv) whereas SEALDH-II
138 is a wide-range instrument(3 – 40000 ppmv),it is nevertheless evident that the large overlap region (from 5
139 to 150 ppmv) between our validation, AquaVIT's, and SEALDH-II's concentration range will allow to infer
140 new and sustainable statements from our validation results.

141 Therefore, we present in this paper the first comparison of an airborne hygrometer (SEALDH-II) with a
142 metrological standard for the atmospheric relevant gas pressure (65 – 950 hPa) and H₂O mole fraction range
143 (5 – 1200 ppmv). We will discuss the validation setup, procedure, and results. Based on this validation,
144 SEALDH-II is by definition the first airborne transfer standard for water vapor which links laboratory and
145 field campaigns directly to metrological standards.

146

147 **2. SEALDH-II**

148 **2.1. System description**

149 This paper focuses on the metrological accuracy validation of the **Selective Extractive Airborne Laser Diode**
150 **Hygrometer (SEALDH-II)**. SEALDH-II is the airborne successor of the proof-of-concept spectrometer
151 (SEALDH-I) study published in (Buchholz et al., 2014), which showed the possibility and the achievable
152 accuracy level for calibration-free dTDLAS hygrometry. The publication (Buchholz et al., 2014)
153 demonstrates this for the 600 ppmv to 20000 ppmv range at standard ambient pressure. The instruments
154 SEALDH-I, SEALDH-II and also HAI (Buchholz et al., 2017) are all three built with the design philosophy
155 that every single reported value of the instrument should have a “related boundary/operation condition
156 snap shot” allowing to exclude the possibility of any instrumental malfunction during the measurement.
157 SEALDH-II is from this perspective the most extensive approach (capturing much more boundary
158 condition data (Buchholz et al., 2016)), while HAI can serve as a multi-channel, multi-phase hygrometer for
159 a broader variety of scientific questions.

160 SEALDH-II integrates numerous different principles, concepts, modules, and novel parts, which contribute
161 to or enable the results shown in this paper. SEALDH-II is described in detail in (Buchholz et al., 2016). The
162 following brief description covers the most important technical aspects of the instrument from a user’s
163 point of view:

164 SEALDH-II is a compact (19” rack 4 U (=17.8 cm)) closed-path, absolute, directly Tunable Diode Laser
165 Absorption Spectroscopy (dTDLAS) hygrometer operating at 1.37 μm . With its compact dimensions and the
166 moderate weight (24 kg), it is well suited for space- and weight-limited airborne applications. The internal
167 optical measurement cell is a miniaturized White-type cell with an optical path length of 1.5 m (Kühnreich
168 et al., 2016; White, 1976). It is connected to the airplane’s gas inlet via an internal gas handling system
169 comprising a temperature exchanger, multiple temperature sensors, a flow regulator, and two gas pressure
170 sensors.

171 Approximately 80 different instrument parameters are controlled, measured, or corrected by SEALDH-II at
172 any time to provide an almost complete supervision and detection of the spectrometer status – we termed
173 this concept “holistic dTDLAS spectroscopy”(Buchholz and Ebert, 2014a). This extensive set of monitoring
174 data ensures reliable and well-characterized measurement data at any time. The knowledge about the
175 instruments status strongly facilitates metrological uncertainties calculations. SEALDH-II’s calculated linear
176 part of the measurement uncertainty is 4.3%, with an additional offset uncertainty of ± 3 ppmv (further
177 details in (Buchholz et al., 2016)). The precision of SEALDH-II was determined via the Allan-variance
178 approach and yielded 0.19 ppmv ($0.17 \text{ ppmv}\cdot\text{m}\cdot\text{Hz}^{-1/2}$) at 7 Hz repetition rate and an ideal precision of 0.056
179 ppmv ($0.125 \text{ ppmv}\cdot\text{m}\cdot\text{Hz}^{-1/2}$) at 0.4 Hz. In general, SEALDH-II’s time response is limited by the gas flow
180 through the White-type multi-pass measurement cell with a volume of 300 ml. With the assumption of a
181 bulk flow of 7 SLM at 200 hPa through the cell, the gas exchange time is 0.5 seconds.

182 SEALDH-II's measurement range covers 3 – 40000 ppmv. The calculated mixture fraction offset uncertainty
 183 of ± 3 ppmv defines the lower detection limit. This offset uncertainty by itself is entirely driven by the
 184 capability of detecting and minimizing parasitic water vapor absorption. The concept, working principle,
 185 and its limits are described in (Buchholz and Ebert, 2014b). The upper limit of 40000 ppmv is defined by the
 186 lowest internal instrument temperature, which has to always be higher than the dew point temperature to
 187 avoid any internal condensation. From a spectroscopic perspective, SEALDH-II could handle mole fractions
 188 up to approx. 100000 ppmv before spectroscopic problems like saturation limit the accuracy and increase
 189 the relative uncertainty beyond 4.3%.

190 2.1. Calibration-free evaluation approach

191 SEALDH-II's data treatment works differently from nearly all other published TDLAS spectrometers.
 192 Typically, instruments are setup in a way that they measure the absorbance or a derivative measurand of
 193 absorbance, and link it to the H₂O mole fraction. This correlation together with a few assumptions about
 194 long-term stability, cross interference, gas temperature dependence, gas pressure dependence is enough to
 195 calibrate a system (Muecke et al., 1994). Contrarily, a calibration-free approach requires a fully featured
 196 physical model describing the absorption process entirely. The following description is a brief overview; for
 197 more details see e.g. (Buchholz et al., 2014, 2016; Ebert and Wolfrum, 1994; Schulz et al., 2007).

198 In a very simplified way, our physical absorption model uses the *extended* Lambert-Beer equation (1) which
 199 describes the relationship between the initial light intensity $I_0(\lambda)$ before the absorption path (typically being
 200 in the few mW-range) and the transmitted light intensity $I(\lambda)$.

$$201 \quad I(\lambda) = E(t) + I_0(\lambda) \cdot Tr(t) \cdot \exp[-S(T) \cdot g(\lambda - \lambda_0) \cdot N \cdot L] \quad (1)$$

202 The parameter $S(T)$ describes the line strength of the selected molecular transition. In SEALDH-II's case, the
 203 spectroscopic multi-line fit takes into account 19 transition lines in the vicinity of the target line at 1370 nm
 204 (energy levels: 110 – 211, rotation-vibrational combination band). The other parameters are the line shape
 205 function $g(\lambda - \lambda_0)$, the absorber number density N , the optical path length L and corrections for light-type
 206 background radiation $E(t)$ and broadband transmission losses $Tr(t)$.

207 Equation (1) can be enhanced with the ideal gas law to calculate the H₂O volume mole fraction c :

$$208 \quad c = -\frac{k_B \cdot T}{S(T) \cdot L \cdot p} \int \ln \left(\frac{I(v) - E(t)}{I_0(v) \cdot Tr(t)} \right) \frac{dv}{dt} dt \quad (2)$$

209 The additional parameters in equation (2) are: constant entities like the Boltzmann constant k_B ; the optical
 210 path length L ; molecular constants like the line strength $S(T)$ of the selected molecular transition; the
 211 dynamic laser tuning coefficient $\frac{dv}{dt}$, which is a constant laser property; continuously measured entities such
 212 as gas pressure (p), gas temperature (T) and photo detector signal of the transmitted light intensity $I(v)$ as
 213 well as the initial light intensity $I_0(v)$, which is retrieve during the evaluation process from the transmitted
 214 light intensity $I(v)$.

215 Equation (2) facilitates an evaluation of the measured spectra without any instrument calibration at any
216 kind of water vapor reference (Buchholz et al., 2014; Ebert and Wolfrum, 1994; Schulz et al., 2007) purely
217 based on first principles. Our concept of a fully calibration-free data evaluation approach (this excludes also
218 any referencing of the instrument to a water standard in order to correct for instrument drift, offsets,
219 temperature dependence, pressure dependence, etc.) is crucial for the assessment of the results described in
220 this publication. It should be noted that the term “calibration-free” is frequently used in different
221 communities with dissimilar meanings. We understand this term according to the following quote (JCGM
222 2008, 2008): “calibration (...) in a first step, establishes a relation between the measured values of a quantity
223 with measurement uncertainties provided by a measurement standard (...), in a second step, [calibration]
224 uses this information to establish a relation for obtaining a measurement result from an indication (of the
225 device to be calibrated)”. Calibration-free in this sense means, that SEALDH-II does not use any
226 information from “calibration-, comparison-, test-, adjustment-” runs with respect to a higher accuracy
227 “water vapor standard” to correct or improve any response function of the instrument. SEALDH-II uses as
228 described in (Buchholz et al., 2016) only spectroscopic parameters and the 80 supplementary parameters as
229 measurement input to calculate the final H₂O mole fraction. The fundamental difference between a
230 calibration approach and this stringent concept is that only effects which are part of our physical model are
231 taken into account for the final H₂O mole fraction calculation. All other effects like gas pressure or
232 temperature dependencies, which cannot be corrected with a well-defined physical explanation, remain in
233 our final results even if this has the consequence of slightly uncorrected results deviations. This strict
234 philosophy leads to measurements which are very reliable with respect to accuracy, precision and the
235 instrument’s over-all performance. The down-side is a relatively computer-intensive, sophisticated
236 evaluation. As SEALDH-II stores all the raw spectra, one could – if needed for whatever reason – also
237 calibrate the instrument by referencing it to a high accuracy water vapor standard and transfer the better
238 accuracy e.g. of a metrological standard onto the instrument. Every calibration-free instrument can be
239 calibrated since pre-requirements for a calibration are just a subset of the requirements for a calibration-free
240 instrument. However, a calibration can only improve the accuracy for the relatively short time between two
241 calibration-cycles by adding all uncertainty contributions linked to the calibration itself to the system. This
242 is unpleasant or even intolerable for certain applications and backs our decision to develop a calibration-
243 free instrument to enable a first principle, long-term stable, maintenance-free and autonomous hygrometer
244 for field use e.g. at remote sites or aircraft deployments.

245 **3. SEALDH-II validation facility**

246 **3.1. Setup**

247 Figure 1 right shows the validation setup. As a well-defined and highly stable H₂O vapor source, we use a
248 commercial Thunder scientific model (TSM) 3900, similar to (Thunder-Scientific, 2016). This source
249 saturates pre-dried air at an elevated gas pressure in an internally ice-covered chamber. The gas pressure in

250 the chamber and the chamber's wall temperature are precisely controlled and highly stable and thus define
251 the absolute water vapor concentration via the Sonntag equation (Sonntag, 1990). After passing through the
252 saturator, the gas expands to a pressure suitable for the subsequent hygrometer. The pressure difference
253 between the saturation chamber pressure and the subsequent step give this principle its name "two
254 pressure generator". The stable H₂O mole fraction range of the TSM is 1 – 1300 ppmv for these specific
255 deployment conditions. This generator provides a stable flow of approximately 4 – 5 SLM. Roughly 0.5 SLM
256 are distributed to a frost/dew point hygrometer, D/FPH, (MBW 373) (MBW Calibration Ltd., 2010).
257 SEALDH-II is fed with approx. 3.5 SLM, while 0.5 SLM are fed to an outlet. This setup ensures that the dew
258 point mirror hygrometer (DPH)² operates close to the ambient pressure, where its metrological primary
259 calibration is valid, and that the gas flow is sufficiently high in any part of the system to avoid recirculation
260 of air. The vacuum pump is used to vary the gas pressure in SEALDH-II's cell with a minimized feedback
261 on the flow through the D/FPH and the TSM. This significantly reduces the time for achieving a stable
262 equilibrium after any gas pressure change in SEALDH-II's chamber. SEALDH-II's internal electronic flow
263 regulator limits the mass flow at higher gas pressures and gradually opens towards lower pressures
264 (vacuum pumps usually convey a constant volume flow i.e., the mass flow is pressure dependent). We
265 termed this entire setup "traceable humidity generator", THG, and will name it as such throughout the text.

266 3.1. Accuracy of THG

267 The humidity of the gas flow is set by the TSM generator but the absolute H₂O values are traceably
268 determined with the dew point mirror hygrometer (D/FPH). The D/FPH, with its primary calibration, thus
269 guarantees the absolute accuracy in this setup. The D/FPH is not affected by the pressure changes in
270 SEADLH-II's measurement cell and operates at standard ambient gas pressure and gas temperature where
271 its calibration is most accurate. The D/FPH was calibrated (Figure 2) at the German national standard for
272 mid-range humidity (green, 600 – 8000 ppmv) as well as at the German national standard for low-range
273 humidity (blue, for lower values 0.1 – 500 ppmv). The two national standards work on different principles:
274 The two pressure principle (Buchholz et al., 2014) currently supplies the lower uncertainties (green, "±"-
275 values in Figure 2). Uncertainties are somewhat higher for the coulometric generator (Mackrodt, 2012) in
276 the lower humidity range (blue). The "Δ"-values in Figure 2 show the deviations between the readings of
277 the D/FPH and the "true" values of the national primary standards.

² The used dew point mirror hygrometer can measure far below 0°C; therefore, it is a dew point mirror above > 0°C and a frost point mirror as soon as there is ice on the mirror surface. We will use both DPH and D/FPH abbreviations interchangeably.

278 **4. SEALDH-II validation procedure**

279 **4.1. Mid-term multi-week permanent operation of SEALDH-II**

280 One part of the validation was a permanent operation of SEALDH-II over a time scale much longer than the
281 usual air or ground based scientific campaigns. In this paper, we present data from a permanent 23 day
282 long (550 operation hours) operation in automatic mode. Despite a very rigorous and extensive monitoring
283 of SEALDH-II's internal status, no malfunctions of SEALDH-II could be detected. One reason for this are
284 the extensive internal control and error handling mechanisms introduced in SEALDH-II, which are
285 mentioned above and described elsewhere (Buchholz et al., 2016). Figure 3 shows an overview of the entire
286 validation. The multi-week validation exercise comprises 15 different H₂O mole fraction levels between 2
287 and 1200 ppmv. At each mole fraction level, the gas pressure was varied in six steps (from 65 to 950 hPa)
288 over a range which is particularly interesting for instruments on airborne platforms operating from
289 troposphere to lower stratosphere where SEALDH-II's uncertainty ($4.3\% \pm 3$ ppmv) is suitable. Figure 3
290 (top) shows the comparison between SEALDH-II (black line) and the THG setup (red). Figure 3 (bottom)
291 shows the gas pressure (blue) and the gas temperature (green) in SEALDH-II measurement cell. The gas
292 temperature increase in the second week was caused by a failure of the laboratory air conditioner that led to
293 a higher room temperature and thus higher instrument temperature. Figure 4 shows the 200 hPa section of
294 the validation in Figure 3. To avoid any dynamic effects from time lags, hysteresis of the gas setup, or the
295 instruments themselves, every measurement at a given mole fraction/pressure combination lasted at least
296 60 min. The data from the THG (red) show that there is nearly no feedback of a gas pressure change in
297 SEALDH-II's measurement cell towards the D/FPH, respectively the entire THG. The bottom subplot in
298 Figure 4 shows the relative deviation between the THG and SEALDH-II. This deviation is correlated to the
299 absolute gas pressure level and can be explained by deficiencies of the Voigt lines shape used to fit
300 SEALDH-II's spectra (Buchholz et al., 2014, 2016). The Voigt profile, a convolution of Gaussian (for
301 temperature broadening) and Lorentzian (pressure broadening) profiles used for SEALDH-II's evaluation,
302 does not include effects such as Dicke Narrowing, which become significant at lower gas pressures.
303 Neglecting these effects cause systematic, but long-term stable and fully predictable deviations from the
304 reference value in the range from sub percent at atmospheric gas pressures to less than 5 % at the lowest gas
305 pressures described here. We have chosen not to implement any higher order line shape (HOLS) models as
306 the spectral reference data needed are not available at sufficient accuracy. Further, HOLS would force us to
307 increase the number of free fitting parameters, which would destabilize our fitting procedure, and lead to
308 reduced accuracy/reliability (i.e., higher uncertainty) as well as significantly increased computational
309 efforts. This is especially important for flight operation where temporal H₂O fluctuations (spatial
310 fluctuations result in temporal fluctuations for a moving device) occur with gradients up to 1000 ppmv/s.
311 These well understood, systematic pressure dependent deviations will be visible in each further result plot
312 of this paper. The impact and methods of compensation are already discussed in (Buchholz et al., 2014). The
313 interested reader is referred to this publication for a more detailed analysis and description.

314 SEALDH-II's primary target areas of operations are harsh field environments. Stability and predictability is
315 to be balanced with potential, extra levels of accuracy which might not be required or reliably achievable
316 for the intended application. Higher order line shape models are therefore deliberately traded for a stable,
317 reliable, and unified fitting process under all atmospheric conditions. This approach leads to systematic,
318 predictable deviations in the typical airborne accessible atmospheric gas pressure range (125 – 900 hPa) of
319 less than 3%. One has to compare these results for assessment to the non-systematic deviations of 20%
320 revealed during the mentioned AquaVIT comparison campaign (Fahey et al., 2014). Hence, for
321 field/airborne purposes, the 3% instrument uncertainty seems to be fully acceptable – especially in airborne
322 environments where the water vapor content is locally very inhomogeneous (leads to rapid temporal
323 variations) and therefore the sampling system enhances the instrument uncertainty significantly.
324 This comparison with AquaVIT should just provide a frame to embed the 3%. The H₂O mole fraction range
325 of Aquavit (0 – 150 ppmv) versus this validation range (5 -1200 ppmv) and the instruments configuration at
326 AquaVIT (mainly (upper) stratospheric hygrometers) versus SEALDH-II as a wide range instrument (3 –
327 40000 ppmv) do not allow a direct comparison. Sadly, there is no other reliable (representative for the
328 community, externally reviewed, blind submission, etc.) comparison exercise such as AquaVIT for higher
329 concentration ranges.

330 **4.1. Assessment of SEALDH-II's mid-term accuracy: Dynamic effects**

331 Besides the pressure dependence discussed above, SEALDH-II's accuracy assessment is exacerbated by the
332 differences in the temporal behavior between the THG's dew/frost point mirror hygrometer (D/FPH) and
333 SEALDH-II: Figure 5 (left) shows an enlarged 45 min. long section of measured comparison data. SEALDH-
334 II (black) shows a fairly large water vapor variation compared to the THG (red). The precision of SEALDH-
335 II (see chapter 2) is 0.056 ppmv at 0.4 Hz (which was validated at a H₂O mole fraction of 600 ppmv
336 (Buchholz et al., 2016)) yielding a signal to noise ratio of 10700. Therefore, SEALDH-II can very precisely
337 detect variations in the H₂O mole fraction. Contrarily, the working principle of a D/FPH requires an
338 equilibrated ice/dew layer on the mirror. Caused by the inertial thermal adjustment process, the response
339 time of a dew/frost point mirror hygrometer has certain limitations due to this principle (the dew/frost
340 point temperature measurement is eventually used to calculate the final H₂O mole fraction), whereas the
341 optical measurement principle of SEALDH-II is only limited by the gas transport, i.e., the flow (exchange
342 rate) through the measurement cell. The effect of those different response times is clearly visible from 06:00
343 to 06:08 in Figure 5. The gas pressure of SEALDH-II's measurement cell (blue), which is correlated to the
344 gas pressure in the THG's ice chamber, shows an increase of 7 hPa – caused by the regulation cycle of the
345 THG's generator (internal saturation chamber gas pressure change). The response in the THG frost point
346 measurement (green, red) shows a significant time delay compared to SEALDH-II, which detects changes
347 approx. 20 seconds faster. This signal delay is also clearly visible between 06:32 to 06:40, where the water
348 vapor variations detected by SEALDH-II are also visible in the smoothed signals of the THG. Figure 5 right
349 shows such a variation in detail (5 min). The delay between the THG and SEALDH-II is here also
350 approximately 20 seconds. If we assume that SEALDH-II measures (due to its high precision) the true water

351 vapor fluctuations, the relative deviation can be interpreted as overshooting and undershooting of the
352 D/FPH's controlling cycle, which is a commonly known response behavior of slow regulation feedback
353 loops to fast input signal changes. The different time responses lead to "artificial" noise in the mole fraction
354 differences between SEALDH-II and THG. Theoretically, one could characterize this behavior and then try
355 to correct/shift the data to minimize this artificial noise. However, a D/FPH is fundamentally insufficient for
356 a dynamic characterization of a fast response hygrometer such as SEALDH-II. Thus, the better strategy is to
357 keep the entire system as stable as possible and calculate mean values by using the inherent assumption
358 that under- and overshoots of the DPM affect the mean statistically and equally. With this assumption, the
359 artificial noise can be seen in the first order as Gaussian distributed noise within each pressure step (Figure
360 4) of at least 60 min. The error induced by this should be far smaller than the above discussed uncertainties
361 of the THG (and SEALDH-II).

362

363 **5. Results**

364 The results of this validation exercise are categorized in three sections according to the following conditions
365 in atmospheric regions: mid-tropospheric range: 1200 – 600 ppmv (Figure 6), upper tropospheric range: 600
366 – 20 ppmv (Figure 7), and lower stratospheric range: 20 – 5 ppmv (Figure 8). This categorization is also
367 justified by the relative influence of SEALDH-II's calculated offset uncertainty of ± 3 ppmv (Buchholz and
368 Ebert, 2014b): At 1200 ppmv, its relative contribution of 0.25% is negligible compared to the 4.3% linear part
369 of the uncertainty of SEALDH-II. At 5 ppmv, the relative contribution of the offset uncertainty is 60% and
370 thus dominates the linear part of the uncertainty. Before assessing the following data, it should be
371 emphasized again that SEALDH-II's spectroscopic first-principles evaluation was designed to rely on
372 accurate spectral data instead of a calibration. SEALDH-II was never calibrated or referenced to any kind of
373 reference humidity generator or sensor.

374 **5.1. The 1200 – 600 ppmv range**

375 Figure 6 shows the summary of the pressure dependent validations in the 1200 – 600 ppmv range. Each of
376 the 48 data points represents the mean over one pressure measurement section of at least 60 min (see Figure
377 4). A cubic polynomial curve fitted to the 600 ppmv results (blue) serves as an internal quasi-reference to
378 connect with the following graphs. The 600 ppmv data (grey) are generated via a supplementary
379 comparison at a different generator: The German national primary mid-humidity generator (PHG). This
380 primary generator data at 600 ppmv indicate a deviation between PHG and THG of about 0.35 %, which is
381 compatible with the uncertainties of the THG (see chapter 3.1) and the PHG (0.4%) (Buchholz et al., 2014).
382 The PHG comparison data also allow a consistency check between the absolute values of (see Figure 2) the
383 PHG (calibration-free), the THG (DPM calibrated) and SEALDH-II (calibration-free).

384 **5.2. The 600 – 20 ppmv range**

385 In this range, the linear part of the uncertainty (4.3%) and the offset uncertainty (± 3 ppmv) have both a
386 significant contribution. Figure 7 shows a clear trend: The lower the mole fraction, the higher the deviation.
387 We believe this is being caused by SEALDH-II's offset variation and will be discussed in the 20 – 5 ppmv
388 range.

389 **5.3. The 20 – 5 ppmv range**

390 The results in this range (Figure 8) are dominated by the offset uncertainty. It is important to mention at this
391 point, that the ± 3 ppmv uncertainties are calculated based on assumptions, design innovations, and several
392 independent, synchronous measurements which are automatically done while the instrument is in
393 operation mode (see publication (Buchholz et al., 2016; Buchholz and Ebert, 2014b)). Hence, the calculated
394 uncertainties resemble an upper uncertainty threshold; the real deviation could be lower than 3 ppmv. A
395 clear assessment is fairly difficult since at low concentrations (i.e., low optical densities) several other effects
396 occur together such as, e.g., optical interference effects like fringes caused by the very long coherence length
397 of the used laser. However, Figure 9 (left) allows a rough assessment of the offset instability. This plot
398 shows all the data below 200 ppmv, grouped by the gas pressure in the measurement cell. If one ignores the
399 65 hPa and 125 hPa measurements, which are clearly affected by higher order line shape effects (see above),
400 the other measurements fit fairly well in a ± 1 ppmv envelope function (grey). In other words, SEALDH-II's
401 combined offset "fluctuations" are below 1 ppmv H₂O. All validation measurements done with SEALDH-II
402 during the last years consistently demonstrated a small offset variability so that the observed offset error is
403 around 0.6 ppmv – i.e., only 20% of the calculated ± 3 ppmv.

404 **5.4. General evaluation**

405 Figure 9 presents a summary of all 90 analyzed mole fraction/pressure-pairs during the 23 days of
406 validation. The calculated uncertainties (linear 4.3% and offset ± 3 ppmv) of SEALDH-II are plotted in
407 purple. This uncertainty calculation doesn't include line shape deficiencies and is therefore only valid for a
408 pressure range where the Voigt profile can be used to represent all major broadening effects of absorption
409 lines (Dicke, 1953; Maddaloni et al., 2010). This is the case above 250 hPa. The results at 950, 750, 500,
410 250 hPa show that the maximum deviations, derived from these measurements, can be described by: linear
411 +2.5%, offset -0.6 ppmv.

412 It should be noted that this result doesn't change the statement about SEALDH-II's uncertainties, since
413 these are calculated and not based on any validation/calibration process. This is a significantly different
414 approach between calibration-free instruments such as SEALDH-II and other classical spectroscopic
415 instruments which rely on sensor calibration. SEALDH-II provides correctness of measurement values
416 within its uncertainties because any effect which causes deviations has to be included in the evaluation
417 model – otherwise it is not possible to correct for it.

418 As mentioned before, any calibration-free instrument can be calibrated too (see e.g. (Buchholz et al., 2013)).

419 However by doing so, one must accept to a certain extent loss of control over the system, especially in
420 environments which are different from the calibration environment. For example, if a calibration was used
421 to remove an instrumental offset, one has to ensure that this offset is long-term stable, which is usually
422 quite difficult, as shown by the example of parasitic water offsets in fiber coupled diode laser hygrometers
423 (Buchholz and Ebert, 2014b). Another option is to choose the recalibration frequency high enough; i.e.,
424 minimizing the drift amplitude by minimizing the time between two calibrations. This, however, reduces
425 the usable measurement time and leads to considerable investment of time and money into the calibration
426 process. For the case of SEALDH-II, a calibration of the pressure dependence – of course tempting and easy
427 to do – would directly “improve” SEALDH-II’s laboratory overall performance level from $\pm 4.3\% \pm 3$ ppmv
428 to $\pm 0.35\% \pm 0.3$ ppmv. At first glance, this “accuracy” would then be an improvement by a factor of 55
429 compared to the mentioned results of AquaVIT (Fahey et al., 2014). However, it is extremely difficult – if
430 not impossible – to guarantee this performance and the validity of the calibration under harsh field
431 conditions; instead SEALDH-II would “suffer” from the same typical calibration associated problems in
432 stability and in predictability. Eventually, the calibration-free evaluation would define the trusted values
433 and the “improvement”, achieved by the calibration, would have to be used very carefully and might
434 disappear eventually.

435 **6. Conclusion and Outlook**

436 The SEALDH-II instrument, a recently developed, compact, airborne, calibration-free hygrometer
437 (Buchholz et al., 2016) which implements a holistic, first-principle, direct tunable diode laser absorption
438 spectroscopy (dTDLAS) approach (Buchholz and Ebert, 2014a) was stringently validated at a traceable
439 water vapor generator at the German national metrology institute (PTB). The pressure dependent
440 validation covered a H₂O range from 5 to 1200 ppmv and a pressure range from 65 hPa to 950 hPa. In total,
441 90 different H₂O mole fraction/pressure levels were studied within 23 days of permanent validation
442 experiments. Compared to other comparisons of airborne hygrometers - such as those studied in the non-
443 metrological AquaVIT campaign (Fahey et al., 2014), where a selection of the best “core” instruments still
444 showed an accuracy scatter of at least $\pm 10\%$ without an absolute reference value - our validation exercise
445 used a traceable reference value derived from instruments directly linked to the international dew-point
446 scale for water vapor. This allowed a direct assessment of SEALDH-II’s absolute performance with a
447 relative accuracy level in the sub percent range. Under these conditions, SEALDH-II showed an excellent
448 absolute agreement within its uncertainties which are 4.3% of the measured value plus an offset of ± 3 ppmv
449 (valid at 1013 hPa). SEALDH-II showed at lower gas pressures - as expected - a stable, systematic, pressure
450 dependent offset to the traceable reference, which is caused by the line shape deficiencies of the Voigt line
451 shape: e.g. at 950 hPa, the systematic deviation of the calibration-free evaluated results could be described
452 by (linear +0.9%, offset -0.5 ppmv), while at 250 hPa the systematic deviations could be described by (linear
453 +2.5%, offset -0.6 ppmv). If we suppress this systematic pressure dependence, the purely statistical
454 deviation is described by linear scatter of $\pm 0.35\%$ and an offset uncertainty of ± 0.3 ppmv.

455 Due to its extensive internal monitoring and correction infrastructure, SEALDH-II is very resilient against a
456 broad range of external disturbances and has an output signal temperature coefficient of only 0.026%/K,
457 which has already been validated earlier (Buchholz et al., 2016). Therefore, these results can be directly
458 transferred into harsh field environments. With this metrological validation presented here, SEALDH-II is
459 the first directly deployable, metrologically validated, airborne transfer standard for atmospheric water
460 vapor. Having already been deployed in several airborne and laboratory measurement campaigns,
461 SEALDH-II thus directly links for the first time, scientific campaign results to the international metrological
462 water vapor scale.

463 For future applications, the measurement path length of 1.5 m and hence SEALDH-II's sensitivity could be
464 relatively quickly enhanced by a factor of 5-10 by implementing a longer path absorption cell. A linear
465 increase of the absorption path yield a proportional scaling of the SEALDH-II's dynamic range (currently at
466 1.5 m: 3 – 40 000 ppmv; lower limit defined by the calculated offset uncertainty of ± 3 ppmv). With this
467 fairly simple adaption SEALDH-II could be adapted to lower H₂O mole fraction ranges, which would make
468 SEALDH-II more suitable for stratospheric applications. The calculated offset uncertainty of SEALDH-II is
469 reciprocally correlated with the optical path-length. Therefore, an increase of the current 1.5 m optical path
470 length to e.g. 30 m or more with different cell designs such as (McManus et al., 1995) or (Tuzson et al., 2013),
471 would allow to reduce the offset uncertainty to 0.15 ppmv; the above discussed laboratory offset deviation
472 performance could reach levels of down to ± 0.015 ppmv.

473

474 **Data availability**

475 *The underlying data for the results shown in this paper are raw spectra (time vs. photo current), which are compressed*
476 *to be compatible with the instruments data storage. In the compressed state the total amount is approximately 6GB of*
477 *binary data. Uncompressed data size is approx. 60 GB. We are happy to share these data on request.*

478

479 **Author Contributions**

480 *Bernhard Buchholz and Volker Ebert conceived and designed the experiments. Bernhard Buchholz performed the*
481 *experiments; Bernhard Buchholz and Volker Ebert analyzed the data and wrote the paper.*

482

483 **Conflicts of Interest**

484 *The authors declare no conflict of interest*

485

486 **Acknowledgements:**

487 *Parts of this work were embedded in the EMPIR (European Metrology Program for Innovation and Research) projects*
488 *METEOMET- 1 and METEOMET-2. The authors want to thank Norbert Böse and Sonja Pratzler (PTB Germany)*
489 *for operating the German primary national water standard and the traceable humidity generator. Last but not least,*
490 *the authors thank James McSpirtt (Princeton University) for the various discussions about reliable sensor designs*
491 *and Mark Zondlo (Princeton University) for sharing his broad knowledge about atmospheric water vapor*
492 *measurements.*

494 **7. References**

- 495 Buchholz, B. and Ebert, V.: Holistic TDLAS spectrometry: The role of comprehensive housekeeping data for
496 robust quality assurance illustrated by two absolute, airborne TDLAS Hygrometers: SEALDH-II and HAI,
497 FLAIR 2014 - F. Laser Appl. Ind. Res., 2014a.
- 498 Buchholz, B. and Ebert, V.: Offsets in fiber-coupled diode laser hygrometers caused by parasitic absorption
499 effects and their prevention, *Meas. Sci. Technol.*, 25(7), 75501, doi:10.1088/0957-0233/25/7/075501, 2014b.
- 500 Buchholz, B., Kühnreich, B., Smit, H. G. J. and Ebert, V.: Validation of an extractive, airborne, compact TDL
501 spectrometer for atmospheric humidity sensing by blind intercomparison, *Appl. Phys. B*, 110(2), 249–262,
502 doi:10.1007/s00340-012-5143-1, 2013.
- 503 Buchholz, B., Böse, N. and Ebert, V.: Absolute validation of a diode laser hygrometer via intercomparison
504 with the German national primary water vapor standard, *Appl. Phys. B*, 116(4), 883–899,
505 doi:10.1007/s00340-014-5775-4, 2014.
- 506 Buchholz, B., Kallweit, S. and Ebert, V.: SEALDH-II—An Autonomous, Holistically Controlled, First
507 Principles TDLAS Hygrometer for Field and Airborne Applications: Design–Setup–Accuracy/Stability
508 Stress Test, *Sensors*, 17(1), 68, doi:10.3390/s17010068, 2016.
- 509 Buchholz, B., Afchine, A., Klein, A., Schiller, C. and Krämer, M.: HAI , a new airborne, absolute, twin dual-
510 channel, multi-phase TDLAS-hygrometer: background, design, setup, and first flight data, *Atmos. Meas.
511 Tech.*, 5194, doi:10.5194/amt-10-35-2017, 2017.
- 512 Busen, R. and Buck, A. L.: A High-Performance Hygrometer for Aircraft Use: Description, Installation, and
513 Flight Data, *J. Atmos. Ocean. Technol.*, 12, 73–84, doi:10.1175/1520-0426(1995)012<0073:AHPHFA>2.0.CO;2,
514 1995.
- 515 Cerni, T. A.: An Infrared Hygrometer for Atmospheric Research and Routine Monitoring, *J. Atmos. Ocean.
516 Technol.*, 11, 445–462, doi:10.1175/1520-0426(1994)011<0445:AIHFAR>2.0.CO;2, 1994.
- 517 Desjardins, R., MacPherson, J., Schuepp, P. and Karanja, F.: An evaluation of aircraft flux measurements of
518 CO₂, water vapor and sensible heat, *Boundary-Layer Meteorol.*, 47(1), 55–69, doi:10.1007/BF00122322, 1989.
- 519 Dicke, R.: The effect of collisions upon the Doppler width of spectral lines, *Phys. Rev.*, 89(2), 472–473,
520 doi:10.1103/PhysRev.89.472, 1953.
- 521 Diskin, G. S., Podolske, J. R., Sachse, G. W. and Slate, T. A.: Open-path airborne tunable diode laser
522 hygrometer, in *Proc. SPIE 4817, Diode Lasers and Applications in Atmospheric Sensing*, vol. 4817, pp. 196–
523 204., 2002.
- 524 Durry, G., Amarouche, N., Joly, L. and Liu, X.: Laser diode spectroscopy of H₂O at 2.63 μm for atmospheric
525 applications, *Appl. Phys. B*, 90(3–4), 573–580, doi:10.1007/s00340-007-2884-3, 2008.
- 526 Ebert, V. and Wolfrum, J.: Absorption spectroscopy, in *OPTICAL MEASUREMENTS-Techniques and
527 Applications*, ed. F. Mayinger, pp. 273–312. [online] Available from:
528 https://link.springer.com/chapter/10.1007%2F978-3-642-56443-7_13, 1994.
- 529 Ebert, V., Fernholz, T., Pitz, H. and Ebert, V.: In-situ monitoring of water vapour and gas temperature in a
530 coal fired power-plant using near-infrared diode lasers, *Laser Appl. to Chem. Environ. Anal.*, 26(SAB4), 4–6,
531 doi:10.1364/LACEA.2000.SaB4, 2000.
- 532 Fahey, D. W., Saathoff, H., Schiller, C., Ebert, V., Peter, T., Amarouche, N., Avallone, L. M., Bauer, R.,
533 Christensen, L. E., Durry, G., Dyroff, C., Herman, R., Hunsmann, S., Khaykin, S., Mackrodt, P., Smith, J. B.,
534 Spelten, N., Troy, R. F., Wagner, S. and Wienhold, F. G.: The AquaVIT-1 intercomparison of atmospheric
535 water vapor measurement techniques, *Atmos. Meas. Tech.*, 7, 3159–3251, doi:10.5194/amtd-7-3159-2014,
536 2014.
- 537 Gurlit, W., Zimmermann, R., Giesemann, C., Fernholz, T., Ebert, V., Wolfrum, J., Platt, U. U. and Burrows, J.
538 P.: Lightweight diode laser spectrometer “ CHILD ” for balloon- borne measurements of water vapor and
539 methane, *Appl. Opt.*, 44(1), 91–102, doi:10.1364/AO.44.000091, 2005.

540 Hansford, G. M., Freshwater, R. A., Eden, L., Turnbull, K. F. V., Hadaway, D. E., Ostanin, V. P. and Jones, R.
541 L.: Lightweight dew-/frost-point hygrometer based on a surface-acoustic-wave sensor for balloon-borne
542 atmospheric water vapor profile sounding, *Rev. Sci. Instrum.*, 77, 014502–014502, doi:10.1063/1.2140275,
543 2006.

544 Heinonen, M., Anagnostou, M., Bell, S., Stevens, M., Benyon, R., Bergerud, R. A., Bojkovski, J., Bosma, R.,
545 Nielsen, J., Böse, N., Cromwell, P., Kartal Dogan, A., Aytekin, S., Uytun, A., Fernicola, V., Flakiewicz, K.,
546 Blanquart, B., Hudoklin, D., Jacobson, P., Kentved, A., Lóio, I., Mamontov, G., Masarykova, A., Mitter, H.,
547 Mnguni, R., Otych, J., Steiner, A., Szilágyi Zsófia, N. and Zvizdic, D.: Investigation of the equivalence of
548 national dew-point temperature realizations in the -50 °C to +20 °C range, *Int. J. Thermophys.*, 33(8–9),
549 1422–1437, doi:10.1007/s10765-011-0950-x, 2012.

550 Held, I. and Soden, B.: Water vapor feedback and global warming, *Annu. Rev. energy Environ.*, 25(1), 441–
551 475, doi:10.1146/annurev.energy.25.1.441, 2000.

552 Helten, M., Smit, H. G. J., Sträter, W., Kley, D., Nedelec, P., Zöger, M. and Busen, R.: Calibration and
553 performance of automatic compact instrumentation for the measurement of relative humidity from
554 passenger aircraft, *J. Geophys. Res. Atmos.*, 103(D19), 25643–25652, doi:10.1029/98JD00536, 1998.

555 Hunsmann, S., Wunderle, K., Wagner, S., Rascher, U., Schurr, U. and Ebert, V.: Absolute, high resolution
556 water transpiration rate measurements on single plant leaves via tunable diode laser absorption
557 spectroscopy (TDLAS) at 1.37 μm , *Appl. Phys. B*, 92(3), 393–401, doi:10.1007/s00340-008-3095-2, 2008.

558 JCGM 2008: JCGM 200 : 2008 International vocabulary of metrology – Basic and general concepts and
559 associated terms (VIM) Vocabulaire international de métrologie – Concepts fondamentaux et généraux et
560 termes associés (VIM), *Int. Organ. Stand.*, 3(Vim), 104, doi:10.1016/0263-2241(85)90006-5, 2008.

561 Joint Committee for Guides in Metrology (JCGM): Evaluation of measurement data - An introduction to the
562 “Guide to the expression of uncertainty in measurement” and related documents, BIPM Bur. Int. des Poids
563 Mes. www.bipm.org, 2009.

564 Karpechko, A. Y., Perlwitz, J. and Manzini, E.: *Journal of Geophysical Research : Atmospheres*, , 1–16,
565 doi:10.1002/2013JD021350, 2014.

566 Kiehl, J. T. and Trenberth, K. E.: Earth’s Annual Global Mean Energy Budget, *Bull. Am. Meteorol. Soc.*,
567 78(2), 197–208, doi:10.1175/1520-0477(1997)078<0197:EAGMEB>2.0.CO;2, 1997.

568 Kley, D. and Stone, E.: Measurement of water vapor in the stratosphere by photodissociation with Ly α
569 (1216 Å) light, *Rev. Sci. Instrum.*, 49(6), 691, doi:10.1063/1.1135596, 1978.

570 Krämer, M., Schiller, C., Afchine, A., Bauer, R., Gensch, I., Mangold, A., Schlicht, S., Spelten, N., Sitnikov,
571 N., Borrmann, S., Reus, M. de and Spichtinger, P.: Ice supersaturations and cirrus cloud crystal numbers,
572 *Atmos. Ocean. Opt.*, 9, 3505–3522, doi:10.5194/acp-9-3505-2009, 2009.

573 Kühnreich, B., Höh, M., Wagner, S. and Ebert, V.: Direct single-mode fibre-coupled miniature White cell for
574 laser absorption spectroscopy, *Rev. Sci. Instrum.*, 87(2), 0–8, doi:10.1063/1.4941748, 2016.

575 Ludlam, F.: Clouds and storms: The behavior and effect of water in the atmosphere. [online] Available
576 from: <http://agris.fao.org/agris-search/search.do?recordID=US8025686> (Accessed 24 May 2014), 1980.

577 Mackrodt, P.: A New Attempt on a Coulometric Trace Humidity Generator, *Int. J. Thermophys.*, 33(8–9),
578 1520–1535, doi:10.1007/s10765-012-1348-0, 2012.

579 Maddaloni, P., Malara, P. and Natale, P. De: Simulation of Dicke-narrowed molecular spectra recorded by
580 off-axis high-finesse optical cavities, *Mol. Phys.*, 108(6), 749–755, doi:10.1080/00268971003601571, 2010.

581 May, R. D.: Open-path, near-infrared tunable diode laser spectrometer for atmospheric measurements of
582 H₂O, *J. Geophys. Res.*, 103(D15), 19161–19172, doi:10.1029/98JD01678, 1998.

583 Maycock, A. C., Shine, K. P. and Joshi, M. M.: The temperature response to stratospheric water vapour
584 changes, *Q. J. R. Meteorol. Soc.*, 137, 1070–1082, doi:10.1002/qj.822, 2011.

585 MBW Calibration Ltd.: MBW 373HX, [online] Available from: [http://www.mbw.ch/wp-](http://www.mbw.ch/wp-content/uploads/2014/11/MBW_373_Datasheet_EN_V2.1.pdf)
586 [content/uploads/2014/11/MBW_373_Datasheet_EN_V2.1.pdf](http://www.mbw.ch/wp-content/uploads/2014/11/MBW_373_Datasheet_EN_V2.1.pdf), 2010.

587 McManus, J., Kebabian, P. and Zahniser, M.: Astigmatic mirror multipass absorption cells for long-path-
588 length spectroscopy, *Appl. Opt.*, 34(18), 3336–3348, doi:10.1364/AO.34.003336, 1995.

589 Meyer, J., Rolf, C., Schiller, C., Rohs, S., Spelten, N., Afchine, A., Zöger, M., Sitnikov, N., Thornberry, T. D.,
590 Rollins, A. W., Bozoki, Z., Tatrai, D., Ebert, V., Kühnreich, B., Mackrodt, P., Möhler, O., Saathoff, H.,
591 Rosenlof, K. H. and Krämer, M.: Two decades of water vapor measurements with the FISH fluorescence
592 hygrometer: A review, *Atmos. Chem. Phys.*, 15(14), 8521–8538, doi:10.5194/acp-15-8521-2015, 2015.

593 Möller, D., Feichter, J. and Herrmann, H.: Von Wolken, Nebel und Niederschlag, in *Chemie über den*
594 *Wolken:… und darunter*, edited by R. Zellner, pp. 236–240, WILEY-VCH Verlag GmbH & Co. KGaA,
595 Weinheim., 2011.

596 Muecke, R. J., Scheumann, B., Slemr, F. and Werle, P. W.: Calibration procedures for tunable diode laser
597 spectrometers, *Proc. SPIE 2112, Tunable Diode Laser Spectrosc. Lidar, DIAL Tech. Environ. Ind. Meas.*,
598 2112, 87–98, doi:10.1117/12.177289, 1994.

599 Ohtaki, E. and Matsui, T.: Infrared device for simultaneous measurement of fluctuations of atmospheric
600 carbon dioxide and water vapor, *Boundary-Layer Meteorol.*, 24(1), 109–119, doi:10.1007/BF00121803, 1982.

601 Peter, T., Marcolli, C., Spichtinger, P., Corti, T., Baker, M. B. and Koop, T.: When dry air is too humid,
602 *Science (80-.)*, 314(5804), 1399–1402, doi:10.1126/science.1135199, 2006.

603 Petersen, R., Crouce, L., Feltz, W., Olson, E. and Helms, D.: WVSS-II moisture observations: A tool for
604 validating and monitoring satellite moisture data, *EUMETSAT Meteorol. Satell. Conf.*, 22, 67–77 [online]
605 Available from: https://amdar.noaa.gov/docs/Petersen_presentation.pdf (Accessed 20 February 2017), 2010.

606 Ravishankara, A. R.: Water Vapor in the Lower Stratosphere, *Science (80-.)*, 337(6096), 809–810,
607 doi:10.1126/science.1227004, 2012.

608 Rollins, A., Thornberry, T., Gao, R. S., Smith, J. B., Sayres, D. S., Sargent, M. R., Schiller, C., Krämer, M.,
609 Spelten, N., Hurst, D. F., Jordan, A. F., Hall, E. G., Vömel, H., Diskin, G. S., Podolske, J. R., Christensen, L.
610 E., Rosenlof, K. H., Jensen, E. J. and Fahey, D. W.: Evaluation of UT/LS hygrometer accuracy by
611 intercomparison during the NASA MACPEX mission, *J. Geophys. Res. Atmos.*, 119,
612 doi:10.1002/2013JD020817, 2014.

613 Roths, J. and Busen, R.: Development of a laser in situ airborne hygrometer (LISAH) (feasibility study),
614 *Infrared Phys. Technol.*, 37(1), 33–38, doi:10.1016/1350-4495(95)00103-4, 1996.

615 Salasmaa, E. and Kostamo, P.: HUMICAP® thin film humidity sensor, in *Advanced Agricultural*
616 *Instrumentation Series E: Applied Sciences*, edited by W. G. Gensler, pp. 135–147, Kluwer., 1986.

617 Scherer, M., Vömel, H., Fueglistaler, S., Oltmans, S. J. and Staehelin, J.: Trends and variability of midlatitude
618 stratospheric water vapour deduced from the re-evaluated Boulder balloon series and HALOE, *Atmos.*
619 *Chem. Phys.*, 8, 1391–1402, doi:10.5194/acp-8-1391-2008, 2008.

620 Schiff, H. I., Mackay, G. I. and Bechara, J.: The use of tunable diode laser absorption spectroscopy for
621 atmospheric measurements, *Res. Chem. Intermed.*, 20(3), 525–556, doi:10.1163/156856794X00441, 1994.

622 Schulz, C., Dreizler, A., Ebert, V. and Wolfrum, J.: Combustion Diagnostics, in *Handbook of Experimental*
623 *Fluid Mechanics*, edited by C. Tropea, A. L. Yarin, and J. F. Foss, pp. 1241–1316, Springer Berlin Heidelberg,
624 Heidelberg., 2007.

625 Sherwood, S., Bony, S. and Dufresne, J.: Spread in model climate sensitivity traced to atmospheric
626 convective mixing, *Nature*, 505(7481), 37–42, doi:10.1038/nature12829, 2014.

627 Silver, J. and Hovde, D.: Near-infrared diode laser airborne hygrometer, *Rev. Sci. Instrum.*, 65, 5, 1691–1694
628 [online] Available from: http://ieeexplore.ieee.org/xpls/abs_all.jsp?arnumber=4991817 (Accessed 25
629 November 2013a), 1994.

630 Silver, J. A. and Hovde, D. C.: Near-infrared diode laser airborne hygrometer, *Rev. Sci. Instrum.*, 65(5),
631 1691–1694, doi:10.1063/1.1144861, 1994b.

632 Smit, H. G. J., Rolf, C., Kraemer, M., Petzold, A., Spelten, N., Neis, P., Maser, R., Buchholz, B., Ebert, V. and
633 Tatrai, D.: Development and Evaluation of Novel and Compact Hygrometer for Airborne Research

634 (DENCHAR): In-Flight Performance During AIRTOSS-I / II Research Aircraft Campaigns, *Geophys. Res.*
635 *Abstr.*, 16(EGU2014-9420), 2014.

636 Sonntag, D.: Important new Values of the Physical Constants of 1968, Vapour Pressure Formulations based
637 on the ITS-90, and Psychrometer Formulae, *Meteorol. Zeitschrift*, 40(5), 340–344, 1990.

638 Thornberry, T. D., Rollins, A. W., Gao, R. S., Watts, L. A., Ciciora, S. J., McLaughlin, R. J. and Fahey, D. W.:
639 A two-channel, tunable diode laser-based hygrometer for measurement of water vapor and cirrus cloud ice
640 water content in the upper troposphere and lower stratosphere, *Atmos. Meas. Tech. Discuss.*, 7(8), 8271–
641 8309, doi:10.5194/amtd-7-8271-2014, 2014.

642 Thunder-Scientific: Model 2500 Two-Pressure Humidity Generator, [online] Available from:
643 www.thunderscientific.com (Accessed 12 May 2016), 2016.

644 Tuzson, B., Mangold, M., Looser, H., Manninen, A. and Emmenegger, L.: Compact multipass optical cell for
645 laser spectroscopy., *Opt. Lett.*, 38(3), 257–9, doi:10.1364/OL.38.000257, 2013.

646 Webster, C., Flesch, G., Mansour, K., Haberle, R. and Bauman, J.: Mars laser hygrometer, *Appl. Opt.*, 43(22),
647 4436–4445, doi:10.1364/AO.43.004436, 2004.

648 White, J.: Very long optical paths in air, *J. Opt. Soc. Am.*, 66(5), 411–416, doi:10.1364/JOSA.66.000411, 1976.

649 Wiederhold, P. R.: *Water Vapor Measurement. Methods and Instrumentation*, Har/Dskt., CRC Press., 1997.

650 Zöger, M., Engel, A., McKenna, D. S., Schiller, C., Schmidt, U. and Woyke, T.: Balloon-borne in situ
651 measurements of stratospheric H₂O, CH₄ and H₂ at midlatitudes, *J. Geophys. Res.*, 104(D1), 1817–1825,
652 doi:10.1029/1998JD100024, 1999a.

653 Zöger, M., Afchine, A., Eicke, N., Gerhards, M.-T., Klein, E., McKenna, D. S., Mörschel, U., Schmidt, U., Tan,
654 V., Tuitjer, F., Woyke, T. and Schiller, C.: Fast in situ stratospheric hygrometers: A new family of balloon-
655 borne and airborne Lyman photofragment fluorescence hygrometers, *J. Geophys. Res.*, 104(D1), 1807–1816,
656 doi:10.1029/1998JD100025, 1999b.

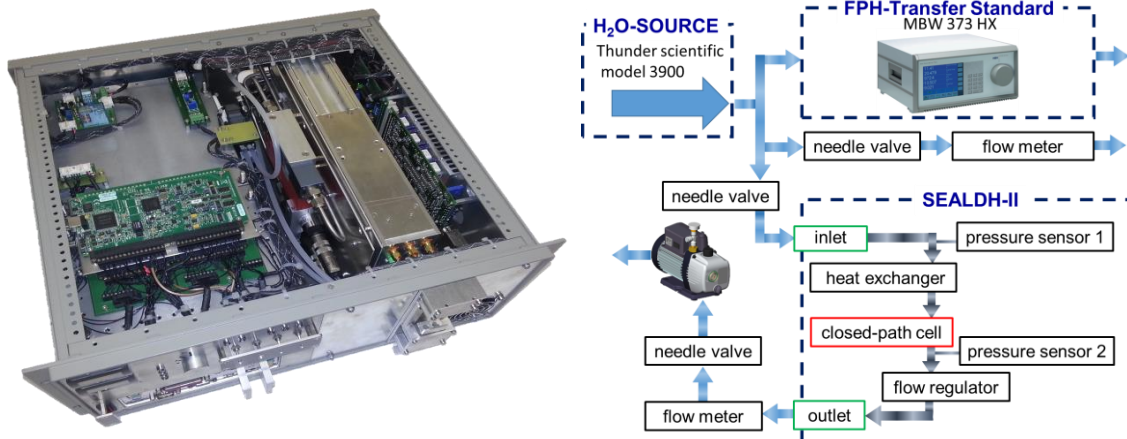
657

658

659 **Figures:**

660

661

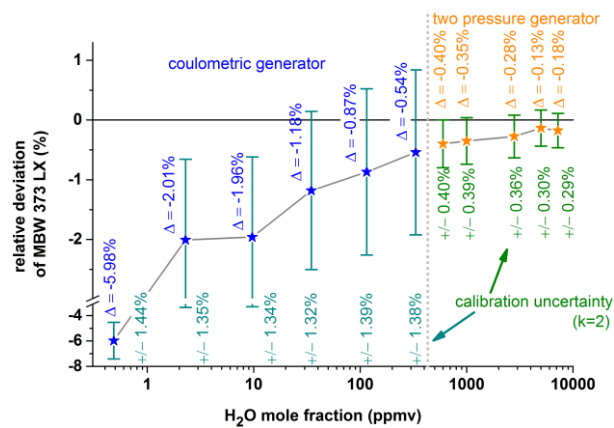


662 Figure 1: Left: Photo of SEALDH-II, the Selective Extractive Airborne Laser Diode Hygrometer (dimension 19" 4 U).
 663 Right: Setup for the metrological absolute accuracy validation. The combination of a H₂O source together with a
 664 traceable dew point hygrometer, DPM, is used as a transfer standard – a traceable humidity generator (THG).
 665

666

667

668

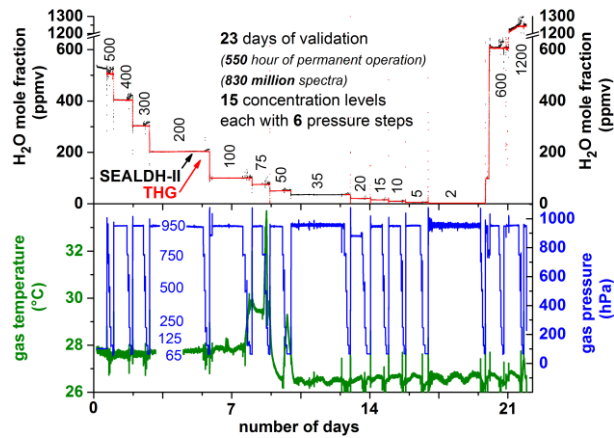


669 Figure 2: Calibration of the DPM (dew/frost point mirror hygrometer, MBW 373 LX, which is used as part of the THG)
 670 at the national primary water vapor standards of Germany. The standard for the higher H₂O mole fraction range
 671 (orange) is a “two pressure generator” (Buchholz et al., 2014); for the lower concentration range (blue) a “coulometric
 672 generator” (Mackrodt, 2012) is used as a reference. The deviations between reference and DPM are labelled with “Δ”.
 673 The uncertainties of every individual calibration point are stated as green numbers below every single measurement
 674 point.
 675

676

677

678



679

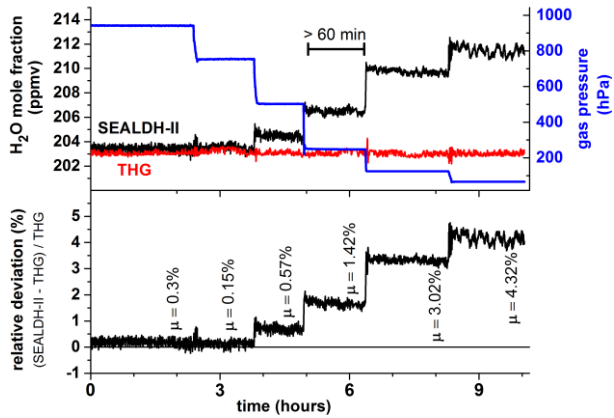
680 Figure 3: Overview showing all data recorded over 23 days of validation experiments. Measurements of the traceable
681 humidity generator (THG) are shown in red, SEALDH-II data in black, gas pressure and gas temperature in SEALDH-
682 II's measurement cell are shown in blue and green. Note: SEALDH-II operated the entire time without any
683 malfunctions; the THG didn't save data in the 35 ppmv section; the temperature increase during the 75 ppmv section
684 was caused by a defect of the air conditioning in the laboratory.

685

686

687

688



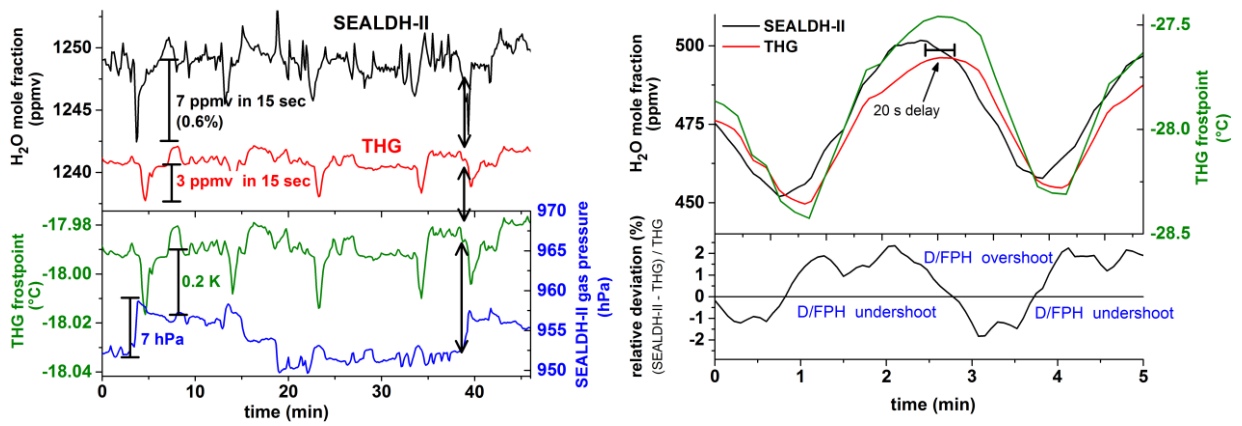
689

690 Figure 4: Detailed plot of the validation at 200 ppmv with six gas pressure steps from 50 to 950 hPa. Each individual
691 pressure level was maintained for at least 60 minutes in order to avoid any dynamic or hysteresis effects and to
692 facilitate clear accuracy assessments. The μ -values define the averaged relative deviation on every gas pressure level.

693

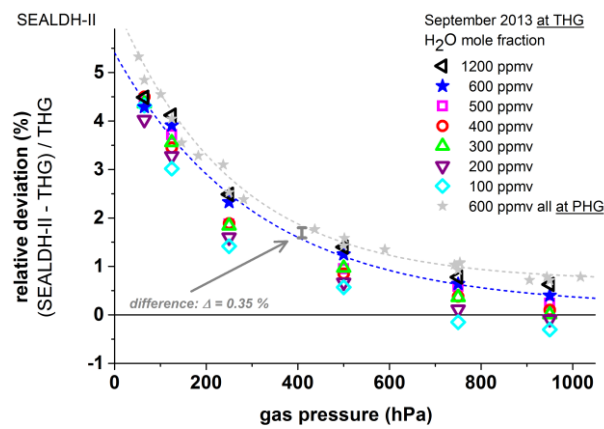
694

695



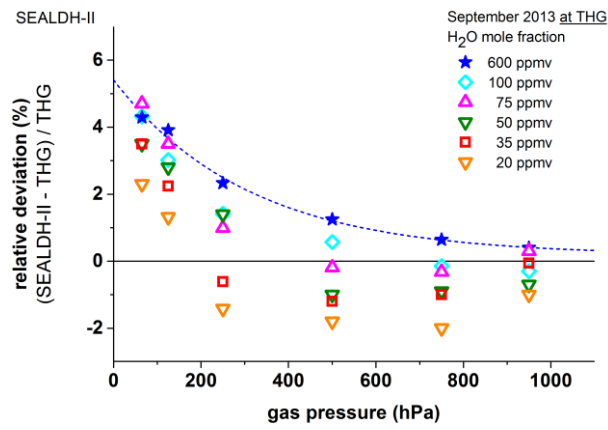
696
 697 Figure 5: Short term H₂O fluctuations in the generated water vapor flow measured by SEALDH-II and the dew/frost
 698 point mirror hygrometer (D/FPH) of the traceable humidity generator (THG). The different dynamic characteristics of
 699 SEALDH-II (fast response time) and THG (quite slow response) lead in a direct comparison to artificial noise.
 700 Oscillating behaviors like in the right figure occur when the THG is not equilibrated. We did not use such data
 701 segments for the accuracy assessments.

702
 703
 704
 705



706
 707 Figure 6: Gas pressure dependent comparison between SEALDH-II and THG over a H₂O mole fraction range from 600
 708 to 1200 ppmv and a pressure range from 50 to 950 hPa. The 600 ppmv values (in grey) are measured directly at the
 709 national primary humidity generator (PHG) of Germany; all other H₂O mole fraction values are measured at and
 710 compared to the traceable humidity generator (THG). All SEALDH-II spectra were evaluated with a calibration-free
 711 first principles evaluation based on absolute spectral parameters. No initial or repetitive calibration of SEALDH-II with
 712 respect to any “water reference” source was used.

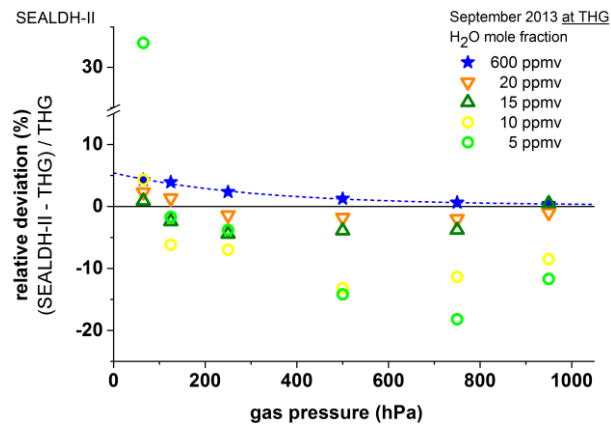
713
 714



715
716 Figure 7: Comparison results as in Figure 6 but for the 200 – 600 ppmv range.

717

718



719
720 Figure 8: Comparison results as in Figure 6 and Figure 7 but for the 5 – 20 ppmv range. All spectra are determined with
721 a calibration-free first principles evaluation concept. The major contribution to the higher fluctuations at lower
722 concentrations is the accuracy of the offset determination (details see text).

723

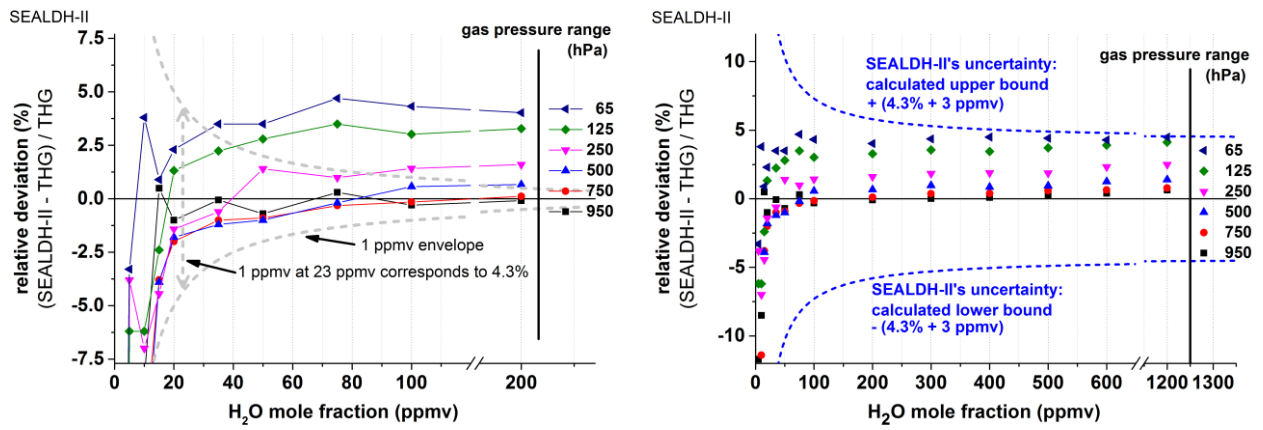


Figure 9: Direct comparison of SEALDH-II versus THG for H₂O mole fractions between 5 and 200 ppmv and gas pressures from 65 to 950 hPa. Both figures show the relative deviations between SEALDH-II and THG grouped and color-coded by gas-pressure. Left plot: relative deviations of SEALDH-II versus THG below 200 ppmv; the grey line indicates the computed relative effect in SEALDH-II's performance caused by ± 1 ppmv offset fluctuation. This line facilitates a visual comparison between an offset impact and the 4.3% linear part of the uncertainty of SEALDH-II. Right plot: relative deviations for all measured data in the same concentration range. Also shown is SEALDH-II's total uncertainty of 4.3% \pm 3 ppmv (calculated for 1013 hPa) as a dashed line.

724

725

726